



# **Tethered Coulomb Structures: Prospects and Challenges**

**Carl R. Seubert and Hanspeter Schaub**

**Simulated Reprint from**

**Journal of the Astronautical Sciences**

**Vol. 57, Nos 1&2, Jan–June, 2009, Pages 347–368**

*A publication of the*  
American Astronautical Society  
AAS Publications Office  
P.O. Box 28130  
San Diego, CA 92198

# Tethered Coulomb Structures: Prospects and Challenges

Carl R. Seubert\* and Hanspeter Schaub†

## Abstract

A Tethered Coulomb Structure (TCS) consists of discrete spacecraft components being joined through a 3D network of physical tethers. The individual components are electrostatically charged to produce repulsive forces between the units. These Coulomb forces assure that the tethers are in tension at all times, and thus maintain a desired large but lightweight spacecraft structure. Coulomb forces are a very recent and novel method of performing relative spacecraft motion control. The spacecraft charge is regulated by emitting electrons or ions, and results in an essentially propellantless force generation method suitable for long-duration missions. The TCS is a new hybrid concept which exploits Coulomb forces to create an inflationary force across the cluster, while the physical tethers control the final spacecraft separation distances. The Coulomb force fields must be large enough to compensate for differential gravitational accelerations and orbital perturbations. A study of expected charge and performance levels is presented. To deploy a TCS, the tethered physical components are first released, and then the Coulomb force fields are engaged to maintain tension. By carefully increasing the tether lengths the TCS size and shape is controlled over time. The TCS concept is discussed. A tether length control concept to stabilize in-plane orientation is discussed using a simple 3D TCS concept.

## Introduction

Large space structures on the order of hundreds of meters have remained an active area of research over the last two decades. The benefit of such structures is that large sensor baselines are achieved providing increased accuracy. This has also led to the more recent research on using free-flying spacecraft formations to achieve the required sensor baselines of multiple kilometers. However, formation flying requires active propulsion methods to maintain a desired cluster shape,

---

\*Graduate Research Assistant, Aerospace Engineering Sciences Department, University of Colorado, Boulder, CO.

†Associate Professor, H. Joseph Smead Fellow, Aerospace Engineering Sciences Department, University of Colorado, Boulder, CO.

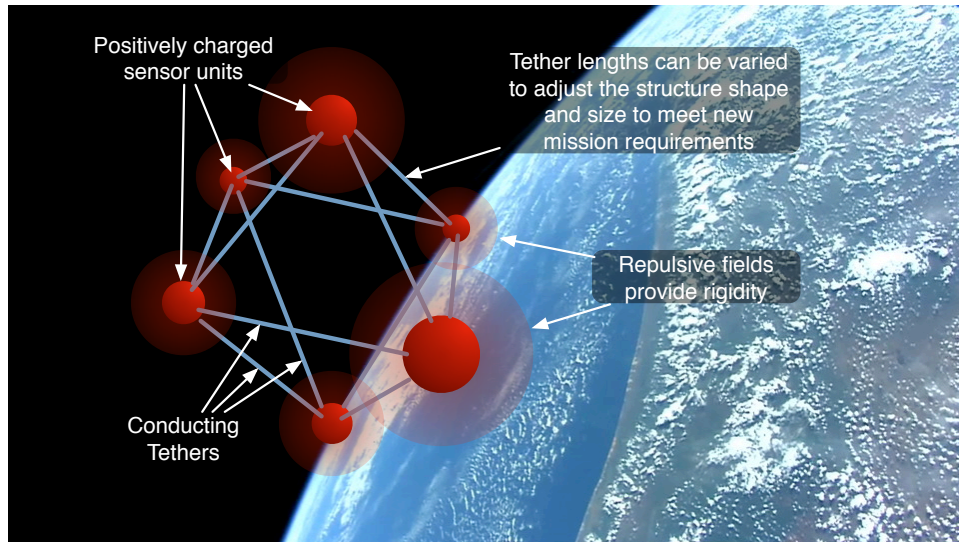


**Figure 1. Tethered Coulomb structure illustration where Coulomb force fields provide tensile forces across the light weight tether structure.**

which poses considerable control and relative motion sensing challenges. In addition, the fuel usage limits the mission life time. Only very simple free-flying spacecraft formations have been demonstrated in space to date.<sup>1,2</sup>

A spacecraft structure requires no fuel to maintain its shape, and thus will have very long mission times in comparison to spacecraft formations. However, developing a light-weight space structure concept hundreds of meters in size is a very daunting task. In particular, such light-weight structures are prone to considerable flexing,<sup>3,4</sup> while the on-orbit assembly challenges provide considerable limitations.<sup>5</sup> The proposed Tethered Coulomb Structure (TCS) concept is illustrated in Figure 1. The TCS is a hybrid blend of formation flying and large structure concepts where discrete charged spacecraft components are joined together through thin tethers whose tension is guaranteed through the repulsive Coulomb forces. Because of the small micro- to milli-Newton levels of tension forces required very thin and light weight tethers are envisioned to limit the relative motion of TCS nodes. Instead of strong conventional kilometer long tethers a spider-web like network of thin threads dozens of meters in length and inextensible are used in this study. Tether spacecraft systems typically only consider a simple two-craft system with a single tether.<sup>6</sup> To maintain tension in the tether the cluster is either spinning,<sup>7,8,9</sup> or using differential gravity or atmospheric drag forces. In particular, Reference 8 discusses a novel 3D tethered structure concept. However, tether tension is maintained in a careful balance of the centripetal and gravity gradient forces.

King et al. in Reference 10 envision a free-flying virtual Coulomb structure 20–30 meters in size, which from Geostationary Earth Orbit (GEO) would provide meter level resolution, hemisphere-wide coverage, and infinite dwell time. At GEO the craft will interact with the local space plasma environment and naturally charge up. By actively emitting positive or negative charge, the on-going

Coulomb thrusting research is investigating how the attractive and repulsive inter-spacecraft forces can be used to control free-flying clusters. This new relative motion control concept can produce small micro- to milli-Newton control forces with  $I_{sp}$  propellant efficiencies up to  $10^{10}$  seconds, and requires only Watt levels of electrical power. The specific impulse,  $I_{sp}$ , is a performance variable that can be used to compare spacecraft propulsion options, as it quantifies the impulse generated per unit mass of propellant.<sup>11</sup> The calculation of  $I_{sp}$  for a Coulomb system is unique as it is calculated here for a two spacecraft system because the force is only generated if more than 1 charged craft are present.

This free-flying spacecraft concept remains an active area of research where the challenging nonlinear and strongly coupled relative orbits must be controlled with limited spacecraft charges. Analytical charged relative equilibria configurations are discussed for 2–4 craft in References 12, 13, 14, while numerical searches have demonstrated charged equilibria with as many as 9 craft.<sup>12</sup> Feedback stabilized virtual Coulomb structures solutions have only been developed for simple 2 craft configurations in orbit,<sup>15, 16, 17, 18</sup> and for circularly spinning 3 craft systems in deep space.<sup>19</sup> The non-affine nature of the charge actuation, as well as the strongly coupled nonlinear equations of motion, makes this a particularly interesting control research problem.

In contrast to the complex guidance and control requirements of a free-flying Coulomb structure, the TCS concept maintains the desired relative positions through the use of both tethers and Coulomb force fields. The physical tethers enforce the desired component separation distances, which results in the TCS having the desired shape. *This provides a tremendous guidance and navigation simplification compared to a free-flying sensor cluster concept, charged or uncharged.* The repulsive Coulomb force fields provide the required tether tension which makes the overall structure act similar to a rigid body. The TCS is similar in concept to the inflatable space structures where a gas provides the required internal pressure for the outer structure to assume a desired shape.<sup>20, 21, 22</sup> The repulsive Coulomb forces result in essentially an inflationary force which provides the tether network with the essential expansion force.

The paper is organized as follows. The TCS concept is laid out discussing how active charge control can provide the required tether tension. The results of a simple study are presented comparing this tension maintenance method to other thruster technologies. The benefits and challenges of the TCS are discussed including how tether length control can be used to deploy the structure, reconfigure its shape and size to meet changing mission requirements, as well as couple with the gravity gradient to influence the orientation. A simple linear tether length control strategy is developed to illustrate how the gravity gradient could be used to stabilize in-plane motion if the structure has a controlled time varying shape. Numerical simulations illustrate the resulting performance.

### Coulomb Thrusting Overview

In space the craft is subjected to the free-flying electrons and ions of the plasma environment. This causes the craft to charge up depending on the plasma temperature, density, and the craft material properties. If operating in sun lit scenario, photons hitting the craft will release electrons from the craft causes an outward photoelectron current as shown in Figure 2. Without charge control the GEO

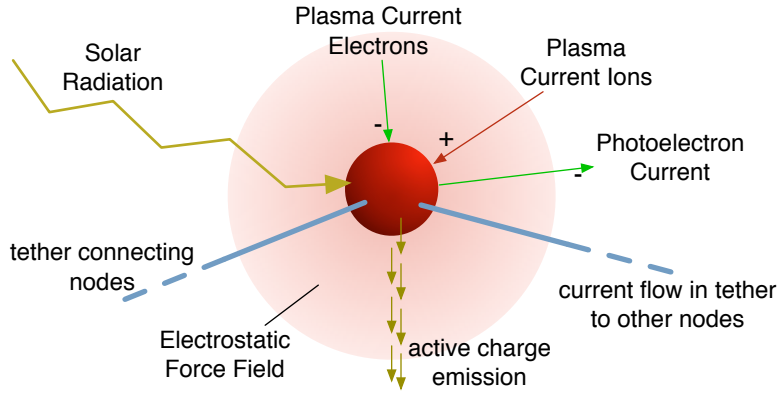


**Figure 2. Charge Balance Illustration of a Spacecraft Subjected to a Plasma Environment with Solar Radiation and Active Charge Control.**

plasma environment will cause the spacecraft potential to vary uncontrolled between positive (sun-lit) and negative (shaded) values. The active charge control is implemented to offset this natural equilibrium to the desired charge levels. Compared to the free-flying Coulomb control concepts, the TCS concept does not require precise charge control. For example, the currently flying CLUSTER mission of 4 spacecraft is employing active charge control to zero their potential with respect to the local space plasma environment.<sup>23,24,25</sup> Here Volt-level precise charge regulation is required to not bias the charged particles sensors. The Coulomb force fields of the TCS concept must simply be strong enough to overcome any differential gravitational or perturbation forces trying to deform the TCS. This greatly simplifies the charge control challenges compared to the untethered Coulomb formation flying concepts. To achieve regulated spacecraft charges and repulse all TCS components, certain structure modules will continuously eject either electrons or ions. By making the tethers conducting, the other spacecraft modules will also be charged without necessarily requiring charge control mechanisms. This could reduce the overall weight and control complexity of the TCS concept compared to tetherless Coulomb force structures. For the GEO mission scenarios considered the electrodynamic (Lorentz) tether forces are several orders of magnitudes smaller than the Coulomb forces. This is due to the GEO spacecraft having essentially zero relative velocity to the already weak Earth's magnetic field.<sup>15</sup> Further, the tethers considered are very short and won't operate as electrodynamic tethers.

The space plasma environment contains free-flying charged particles which partially shield the spacecraft's electrostatic forces from each other. The strength of this shielding is determined through the Debye length  $\lambda_d$ , which is added as an exponential decay to the standard vacuum electrostatic force calculation.<sup>26</sup> The force  $\mathbf{F}_{12}$  experienced between 2 bodies with charges  $q_1$  and  $q_2$  is given by

$$|\mathbf{F}_{12}| = k_c \frac{q_1 q_2}{r_{12}^2} e^{-r_{12}/\lambda_d} \quad (1)$$

where  $k_c = 8.99 \times 10^9 \text{ C}^{-2}\text{Nm}^2$  is the Coulomb constant, and  $r_{12}$  is the separation distance. At GEO and HEO the plasma is hot and sparse enough to yield Debye lengths ranging from 100-1000 meters. This allows Coulomb forces to be effective for inter-spacecraft separation distances up to about 100 meters. However, at Low Earth Orbits (LEO) the plasma Debye length are of the order of centimeter to decimeters,<sup>10,27</sup> making the Coulomb thrusting concept unfeasible at LEO. However, developing large space structures at GEO or deep space is particularly expensive due to the high costs of launching such a structure to a high altitude. Any saving in overall weight yield substantial cost savings.

To maintain a specified charge level with respect to the plasma, the natural current flux to the craft must be offset with active charge emission. Because the TCS nodal separation distances are relative small on the order of dozens of meters, all nodes experience a similar space environment and a similar charge flux to the node. The actual charge accumulated depends on the dimension and surface of the body considered. The larger the craft, the more net charge it will acquire.<sup>10</sup> The net Coulomb force between two bodies is dependent on the charge product as shown in Eq. (1). For a simple spherical shape of radius  $\rho_i$  the charge  $q_i$  results in the potential  $V_i$ :

$$V_i = k_c \frac{q_i}{\rho_i} \quad (2)$$

The larger the potential  $V_i$  is that a node can acquire, the larger the Coulomb force and the associate internal pressure force will be. Very large potentials form a technical challenge in that small charge deviations can lead to discharge and arcing. To reduce the potential the node radii  $\rho_i$  should be increased. However, this increased surface area will require higher charge emission efforts to combat the increased net charge flow to the craft from the plasma environment. This manifests itself in increased Coulomb thrusting power requirements. Let  $I_e$  be the net current flowing into the craft due to the space environment. The power required to maintain a particular potential  $V_i$  is given by<sup>10</sup>

$$P_i = V_i I_e \quad (3)$$

To implement the nodal charge control a balance must be achieved in technically achievable node potentials and power requirements.

To reduce the overall TCS complexity it is feasible to only have select nodes contain active charge emission devices. The potential is then shared using conducting tethers connected to other nodes. While this reduces the overall mechanical complexity of the TCS concept, note that this potential sharing strategy does not reduce the overall power requirement. This is determined through the node dimensions and their exposure to the space environment. If each node contains its charge emission control hardware, the power requirements of each unit are reduced because each node by itself receives a lower net current  $I_e$  from the environment. The benefits of such a strategy include a highly redundant charge control scenario, and the capability to control slight charge variations across the TCS structure.

With ion thrusters such as Field Emission Electric Propulsion (FEEP)<sup>28</sup> or Colloid thrusters<sup>29</sup> the inertial thrust is produced by the momentum exchange of

the expelled ions. This process naturally charges up the spacecraft which is why electrons are also emitted to balance the net current flow from the craft. The CLUSTER mission uses active charge control by using a liquid metal ion source which is essentially a FEEP thruster with a low throttle setting to emit the charge and zero the spacecraft potential with respect to the plasma environment.<sup>30</sup> The proposed TCS charge control process is very similar to these FEEP thrusters. In fact, Makella and King discuss in Reference 31 an important improvement on the FEEP thruster where the sharp ion emitting tip is self-repairing and it is possible to easily switch the thruster from emitting ions or electrons. Thus, such a dual-mode device could be used to perform charge control during nominal operations, and be reset to provide small micro- to milli-Newton levels of *inertial* thrust to perform TCS attitude or continuous station keeping maneuvers.

### TCS Concept Overview

This section discusses the TCS concept and presents the novel features and challenges of such a structure. The aim is not to present final solutions to all these ideas. The goal of this paper is to present TCS as a viable concept and illustrate how these features could enable new classes of space structures.

#### *Large Light-Weight Structures*

The TCS concept envisions a general three-dimensional structure being composed of a discrete set of  $N$  nodes connected through a network of tether cables as illustrated in Figure 3(a). Using either a sub-set of nodes, or by having each node contain active charge emission hardware, repulsive Coulomb force fields are generated to ensure that the tethers remain under tension at all times. Because the Coulomb force strength drops nonlinearly with the separation distance as shown in Eq. (1), the nodal separation distances are kept to 10-100 meters range to avoid excessive node potential requirements. However, large kilometer size structure are still feasible. In this case additional nodes must be included to breach the large dimension and provide sufficient structural control points.

While conventional tethered systems require a nadir alignment or a spinning system to maintain tension, the TCS allows for general three-dimensional tethered space structures to be envisioned. The complex guidance, control and relative motion sensing issues of a free-flying virtual structure are avoided by allowing the tethers to limit the relative motion of the nodes.

Two types of TCSs are envisioned. First Figure 3(a) illustrates a structure where the shape is uniquely defined through the various tether lengths  $L_i$ . The repulsive Coulomb forces ensure that the tethers are under tension at all times. Because the nodal separation distance are relatively small (dozens of meters) compared to conventional tether concepts (multiple-kilometers), the tether segments of the TCS will be relatively stiff. The second TCS type has nodal elements whose positions are not uniquely determined through the tether lengths. Figure 3(b) illustrates a TCS where one primary node has several sub-nodes which are only tethered to this primary node and not to each other. As a result of the mutual repulsive forces the free sub-node will move to a natural equilibrium where these repulsive forces mutually cancel each other. This setup would enable the sub-nodes park next to the primary nodes without strict relative position requirements.

Because the Coulomb forces are internal forces of the TCS, they cannot be used to change the inertial angular momentum of the structure. Certain nodes will require conventional thrusters to apply small  $\Delta v$ 's to perform orbit corrections. Note that these orbit corrections must be subtle such as not to overpower the Coulomb forces and cause the TCS to collapse. Using these thrusters external torques could also be applied to achieve orientational control as illustrated in Figure 3(a).

### *Structure Deployment*

Deploying large space structures poses a particular challenge. The structures are too large to be launched with existing launch vehicles in one piece, human orbit-assembly is very expensive, while autonomous or tele-operated robotic assembly system would also pose additional material that needs to be launched into space. As a result inflatable space structures have been investigated.<sup>20</sup> In particular, on STS 77 the inflatable antenna flight experiment was performed.<sup>32</sup> Here a 14 meter diameter parabolic reflector structure was assembled in orbit by having a gas provide the required internal pressure for the initially compact structure to unfold. However, unless rigidified, such structures are subject to micro-meteorite damage which could cause severe pressure loss. Another approach to achieve larger sensor baselines is to use a Tethered Satellite System (TSS). Here a lightweight cable connects 2 or more nodes and maintains a fixed separation distance. Because the tether can only support tension force, such systems must be released in a particular manner. One option is to have the system be spinning such as the successful Tether Physics and Survivability Satellite Experiment (TiPS). With an initial 4 rpm spin rate, a 37.6 and 10.4 kilogram body achieved a 4 kilometer tether deployment in 42 minutes.\* Another option is to deploy the TSS using a stable relative equilibrium configuration such as a orbit nadir aligned tether. Here the differential gravity provides the required tension. However, such deployments are challenging because the differential gravity force is zero initial and only grows with increasing separation distances. For a two craft, massless tether system the differential radial gravitational force magnitude linearizes to

$$\delta F_r \approx m \frac{3\mu}{r_c^3} L \quad (4)$$

where  $r_c$  is the chief orbit radius,  $\mu$  is the gravitational constant,  $m$  is the node mass, and  $L$  is the tether length.

With the TCS concept the Coulomb forces provide a repulsive force in Eq. (1) from the very beginning even when the separation distance is very small. This greatly simplifies the initial tether deployment compared to conventional TSS concepts. Further, note that tension can be maintained in arbitrary directions if the Coulomb force is large enough to overcome the differential gravity. Consider a TCS consisting of two 100 kg nodes each charged to  $q_i = 1\mu\text{C}$ . For a 1 meter diameter sphere this charge corresponds to 18kV potential. The Debye length  $\lambda_d$  for GEO is set to 200 meters. For an orbit radial (nadir) TCS deployment the resulting tether tension  $T > 0$  is approximated assuming small separation

---

\*see <http://projects.nrl.navy.mil/tips/techspecs.html>

distances by

$$T_{\text{nadir}} = k_c \frac{q_1 q_2}{L^2} e^{-L/\lambda_d} + m \frac{3\mu}{r_c^3} L \quad (5)$$

Figure 5(a) compares the tether tension to the Coulomb and gravity gradient force magnitudes. Note that the gravity gradient assists the Coulomb force in maintaining tensions as the tether length  $L$  increases. However, the Coulomb force provides significant repulsion at very small initial tether lengths. For an along-track deployment there is no gravity gradient force to first order. Here the tether tension is simply equal to the Coulomb repulsion. For a two craft TCS undergoing an orbit normal deployment the gravity gradient force yields a compressive  $\delta F_h$  component.

$$\delta F_h \approx -m \frac{\mu}{r_c^3} L \quad (6)$$

The tether tension is then approximated by

$$T_{\text{normal}} = k_c \frac{q_1 q_2}{L^2} e^{-L/\lambda_d} - m \frac{\mu}{r_c^3} L \quad (7)$$

The forces are compared in Figure 5(b). Note that for tether lengths less than 24 meters the repulsive Coulomb force is sufficient to maintain positive tension. Beyond such orbit normal separation distances this setup requires increased TCS node potentials. Further, please note that these values are only for a very simple 2-craft TCS setup. For more complex three-dimensional TCS configuration with multiple craft the repulsion will be generated through the addition of multiple Coulomb forces.

Note that the required tether tension forces are very small for a GEO TCS concept, and a thin cable would suffice to carry this load. If a cable is used which can rigidize in the space environment (radiation harden), then the Coulomb forces would only be required during the initial inflationary phase of the TCS. Once the networked tether structure assumes the desired shape and the solid tethers can carry small loads of compression, then the charge control would no longer be required.

### *Reconfigurable Shape*

A considerable advantage of the TCS concept compared to other light weight space structures such as the self-inflating space structures is that the TCS shape and size can easily be controlled through time varying tether lengths. No complex mechanical expanding or spherical joints are required to morph a particular structure into another shape. During a shape reconfiguration the charge control must be adjusted to ensure that sufficient cable tension is present. Otherwise the shape is changed using simple kinematic control strategies which determine the required tether length time histories.

Being able to easily modify the shape in a fuel and power efficient strategy opens up new methods for the structure to control the pointing and orientation. For example, a shape could change its aspect ratio to take advantage of a gravity

gradient torque and spin up a formation. Once a particular spin is achieved, the shape could return to a spherical shape to maintain this spin. Or, the shape could be specifically varied to gravity gradient stabilize the orientation of the structure with respect to the orbit nadir axis. Beyond using the gravity gradient to control the orientation, the TCS will require small thrusters which can produce external torques on the structure to reorient it. The FEEP thrusters proposed by Makela and King in Reference 31 are ideal candidates for this task. These devices could be used to both control the spacecraft charge using a low-throttle setting, and through a change in thruster setting be changed to also provide small amounts of inertial thrust.

Because the tether lengths of the TCS concept are rather short, on the order of dozens of meters, they will be relatively inextensible compared to conventional TSS tethers. However, some amount of tether flexing is expected and will result in some small pulsing and flexing of the TCS system. If TCS nodes have individual charge control capabilities, then it is possible to generate small differential charge levels across the structure. These differential forces could be exploited to control the tether flexing and damping such structural modes to zero. This would require more precise charge control capabilities than a simple tether tension maintaining charge control strategy. However, because the goal is to damp structural flexing and remove the associated energy, simple robust Lyapunov optimal damping control methods could be employed to arrest such structural modes.<sup>33</sup> Future work will also include a study of potential tether materials and their consequent elasticity and wrinkling.

### TCS Comparison to Alternate Systems

The TCS concept expected operating regimes are illustrated in Figure 6 as region I. To avoid excessive node electrostatic potentials or voltages, the TCS components are expected to be less than 100 meters apart. Typical envisioned nodal separation distances are on the order of 10-30 meters. Note that kilometer size structures are still envisioned using a network of charged nodes to maintain tether tension throughout the 3D structure. Further, the TCS concept scales easily to having large numbers of sensor nodes due to the relative simplicity of the required charge control system and lack of precise relative motion sensing requirements. Significant charging, and thus electrostatic repulsion, occurs naturally for HEO and GEO spacecraft. The TCS concept exploits this natural perturbation and strengthens it as needed to maintain sufficient tether tension through the structure. However, at Low Earth Orbits (LEO) the space plasma environment effectively shields the Coulomb forces,<sup>10,27</sup> making TCS impractical.

An alternate approach to creating a multitude of sensors positioned precisely relative to each other is to use a free-flying spacecraft formation (region II in Figure 6). Here each craft senses the motion of other craft in the cluster and uses inertial thrusters to control their relative motions. However, thruster plume impingement issues limit such general proximity control to larger separation distances. The ion-engine exhaust is often quite caustic on craft sensors and components. A significant limitation is the difficulty of scaling this concept for a large number of sensor nodes. Currently flying kilometer-size or less formation flying missions often involve two,<sup>1,2</sup> rarely more such as the CLUSTER's mission with four craft.<sup>23</sup> The relative motion sensing and control challenge becomes very sig-

nificant as the number of nodes is increased to the 100s or 1000s such as required for distributed space solar power(SSP)<sup>34</sup> beaming concepts.

A hybrid tether connected structure concept could use fuel efficient micro-thrusters to provide the required tether tension (see region III in Figure 6). This Thrusted Tethered Structure (TTS) concept eliminates the considerable relative motion sensing and control issues of a large cluster of free-flying craft. Tension is maintained even over large distances without requiring spinning or particular orbit equilibrium configurations. However, due to the use of inertial thrusters the separation distances between the nodes must be large to avoid the caustic exhaust plume damaging nearby craft. Further, sufficient fuel and power capabilities must be provided to each tethered structure node. In comparison, the TCS concept only requires certain nodes to be able to create the charge which is then distributed across the conducting tethers. Finally, the nodal thrusting control strategy for a TTS must be carefully balanced such that the net force and torque on the structure is zero. Otherwise, the TTS will experience an orbital or attitude drift. In contrast, the TCS concept produces only cluster internal forces which are guaranteed to not provide a net external force across the structure. The primary benefit of the TTS concept is that it would function in LEO and allow large inter-node separation distances.

**Table 1. Per node one year requirements comparison of the Coulomb and Micro Thruster concepts.**

	Coulomb (Ion/e <sup>-</sup> )	FEEP	Colloid	MicroPPT
Close range exhaust impingement issues	no	yes	yes	yes
Complex guidance and control requirements	no	yes	yes	yes
Long tether length capability	no	yes	yes	yes
Operational altitudes	HEO	LEO-HEO	LEO-HEO	LEO-HEO
1 year fuel mass (grams)	0.01 / 0.00	2.12	21.23	42.46
Electrical Power (Watt)	0.40 / 0.67	0.40	0.05	0.32
$I_{sp}$ (s)	$2.1 \cdot 10^6 / \infty$	$10^4$	$10^3$	500

To compare the expected performance of TCS and TSS concepts, consider two 1 meter diameter spherical spacecraft separated by 25 meters along the orbit normal direction and connected with a ultra fine tether. Note that a conventional tether structure could not establish such a formation because it cannot withstand a compressive force. Assuming 50 kg craft, the differential gravity requires the Coulomb force to provide at least  $6.6 \mu\text{N}$  of continuous thrust to maintain a positive tether tension. This corresponds to a craft charge of  $0.72 \mu\text{C}$ , or a 12.96 kV potential if the craft has a 1 meter diameter. To maintain this force each unit requires only 0.4 Watts of power, while only 0.01 grams of fuel would be required over a year assuming hydrogen ion emission. If renewable electrons are rejected to cause electrostatic repulsion, then the fuel consumed is zero. Table 1 provides a comparison to using FEEP, Colloid and MicroPPT thruster to achieve this ten-

sion. The values in this table are per craft. Note that all these thruster concepts would cause plume impingement issues operating this close to each other. The inert and fuel propulsion mass budget estimated for a 10 node TCS are illustrated in Figure 7.

Non-thrusted tether structures have been investigated extensively over the years. Here the tether tension is maintained either through spinning the structure, or exploiting stable orbital equilibrium configurations.<sup>35,36,37,38</sup> However, these tether structure concepts are limited to either one-dimensional shapes in orbital equilibriums, or two-dimensional shapes which are spinning. The proposed TCS concept is able to generate much more general one-, two- or three-dimensional shapes not feasible with conventional tether structures. For example, the Coulomb force is able to ensure tether tension for the unstable orbital normal equilibrium configuration of two tethered craft.

### Numerical Simulation and Control Study

The TCS concept is demonstrated using a simple mission scenario showing in-plane attitude control. Modeled here is a geostationary TCS that is capable of reconfiguring its shape by adjusting its tether lengths. The intent of the control methodology is to stabilize the orientation of the TCS by varying its tethers and still achieve a steady-state nominal shape. Reference 16 demonstrated the stabilization of a two craft free-flying system by controlling the separation distance with Coulomb charge. In a similar manner this feedback control technique utilizes a shape reconfiguration that manipulates the mass moment of inertia to control orientation. However, whereas Reference 16 uses the spacecraft charge as the control variable, the TCS uses the tether length rate as the control with the charge only being employed to ensure tension. As an example TCS scenario the 6 node tether system is modeled as shown in Figure 8. The TCS nodes are equipped with tether reel mechanisms allowing variation in length along the radial direction. For this study it is assumed the tethers distances remain short and are modeled as a rigid member capable of withstanding tensile forces only without any flex or extension. It is shown in Reference 15 that the largest disturbance torque acting on the TCS at GEO is differential solar drag. The differential solar disturbance torque is orders of magnitude less than the gravity gradient control torque due to the assumption that the TCS is only dozens of meters in size and the nodes are all equivalent dimension. This disturbance torque along with any others has not been included in this concept simulation study, however will be featured in future work.

#### *TCS Parameters*

The spacecraft control simulation is conducted in a geostationary orbit with parameters defined in Table 2. This orbit allows the simulation to be performed under the effective influence of Earth's gravity and in an environment where the Debye length is still large enough to allow Coulomb interaction between nodes. Modeled here is a symmetric TCS comprised of 6 equal mass nodes with tether connections shown in Figure 8(a). This simple configuration is selected as it offers a desired gravity gradient stabilized inertia distribution. The simulation allows rapid development of any nodal number and configured TCS in future work. Also shown in Figure 8(a) is the orbital frame axes  $\mathcal{O} : [\hat{o}_\theta \ \hat{o}_h \ \hat{o}_r]$  which

regardless of attitude and reconfigured length is always located at the center of mass (CM) of this TCS. The 3-2-1 Euler angle sequence yaw ( $\psi$ ), pitch ( $\theta$ ), and roll ( $\phi$ ) is used to describe the orientation of the TCS body-fixed frame  $\mathcal{B}$  :  $[\hat{\mathbf{b}}_1 \hat{\mathbf{b}}_2 \hat{\mathbf{b}}_3]$  relative to the orbit frame  $\mathcal{O}$ .

**Table 2. GEO and spacecraft parameters.**

Simulation Parameter	Variable	Value
GEO Radius (km)	$R_c$	42164
Circular Angular Rate (rad/s)	$\Omega$	$7.2195 \times 10^{-5}$
Debye length (m)	$\lambda_d$	200
Node mass (kg)	$m_i$	100
Node separation from CM along $\hat{\mathbf{b}}_1$ (m)	$l_1$	5
Node separation from CM along $\hat{\mathbf{b}}_2$ (m)	$l_2$	2.5
Reference node separation from CM along $\hat{\mathbf{b}}_3$ (m)	$L_r$	20

With this node/tether configuration and its alignment with the Earth's radial axis, the TCS, if held rigid, is in a orbit configuration that is marginally stabilized by the Earth's gravity gradient torque on each node if treated as a rigid structure. This is maintained provided the principal TCS moments of inertia uphold the following criteria:  $I_{22} > I_{11} > I_{33}$ .<sup>39</sup> If an axi-symmetric configuration with  $I_{22} = I_{11}$  is considered then the gravity gradient torque will still cause marginally stable pitch and roll motions, however the yaw is no longer linearly controlled by the gravity gradient torque. The corresponding moment of inertia for this TCS expressed in the body frame is

$${}^{\mathcal{B}}[I] = 2m_i \text{diag} (2l_2^2 + L^2, 2l_1^2 + L^2, 2l_1^2 + 2l_2^2) \quad (8)$$

Throughout the simulation the inertia matrix  ${}^{\mathcal{B}}[I]$  is defined in body frame components and the notation is simplified to  $[I]$ . The tether force acting between nodes  $i$  and  $j$  is  $T_{ij}$ . The tethers between the internal nodes (3,4,5, and 6) have a fixed length. As shown in Figure 8(b) the TCS is capable of reconfiguration by manipulating the tether lengths to nodes 1 and 2 ( $T_{1j}$  and  $T_{2j}$ ). Nodes 1 and 2 can move along the  $\hat{\mathbf{b}}_3$  axis changing the dimension,  $L$ , from the CM. By using this dimensional manipulation as a control parameter the inertia matrix is time-varying and is expressed in body frame components as

$$\frac{{}^{\mathcal{B}}d}{dt} ([I]) = 4m_i \text{diag}(\dot{L}, L\dot{L}, 0) \quad (9)$$

Figure 8(b) also shows the natural (un-charged) tether internal forces when the TCS is in an equilibrium configuration with  $\mathcal{B} = \mathcal{O}$ . In this configuration nodes 1 and 2 are accelerated outward from the CM due to the gravity gradient torque and orbital motion. This acceleration induces tension on the connecting tethers. Consequently, the four central nodes accelerate toward the CM and their connecting tethers experience a compressive force. By implementing an equal-

polarity charge on all nodes the repulsive Coulomb force can be used to overcome this natural configuration and ensure all tethers experience tension, maintaining a near-rigid structure.

### Linear Control Development

By treating the TCS as a continuous body the rotational equations of motion under the influence of Earth's gravity can be obtained from Euler's equation

$$\dot{\mathbf{H}} = \frac{\mathcal{B}_d}{dt} ([I]) \boldsymbol{\omega} + [I] \frac{\mathcal{B}_d}{dt} (\boldsymbol{\omega}) + [\tilde{\boldsymbol{\omega}}] [I] \boldsymbol{\omega} = \mathbf{L}_g \quad (10)$$

where the angular rate of the body frame relative to the inertial frame  $\mathcal{N}$  :  $[\hat{\mathbf{n}}_x \hat{\mathbf{n}}_y \hat{\mathbf{n}}_z]$  is defined by  $\boldsymbol{\omega} = \boldsymbol{\omega}_{\mathcal{B}/\mathcal{N}}$  and the tilde matrix notation  $[\tilde{\boldsymbol{\omega}}] \mathbf{x} \equiv \boldsymbol{\omega} \times \mathbf{x}$  is used. The linearized gravity gradient torque vector  $\mathbf{L}_g$  developed in Reference 39 is used here. The torque vector components are converted from orbit to body frame components with a 3-2-1 Euler angle direction cosine matrix and simplified to the form

$$\mathbf{L}_g = \frac{3\Omega^2}{2} \begin{bmatrix} (I_{33} - I_{22}) \sin 2\phi \cos^2 \theta \\ (I_{33} - I_{11}) \sin 2\theta \cos \phi \\ (I_{11} - I_{22}) \sin 2\theta \sin \phi \end{bmatrix} \quad (11)$$

where  $\Omega$  is the circular orbit rate given by Kepler's equation

$$\Omega^2 = \frac{GM_e}{R_c^3} \quad (12)$$

Substituting the 3-2-1 Euler angle kinematic differential equations in Eq. (10) and linearizing for small departure angles about a zero 3-2-1 Euler angle attitude orientation the TCS equations of motion are derived.

$$\dot{I}_{11}(\dot{\phi} + \Omega\psi) + I_{11}(\ddot{\phi} - \Omega\dot{\psi}) + (I_{33} - I_{22})(\Omega\dot{\psi} - \Omega^2\phi) = 3\Omega\phi(I_{33} - I_{22}) \quad (13a)$$

$$\dot{I}_{22}(\dot{\theta} + \Omega) + I_{22}\ddot{\theta} = 3\Omega^2\theta(I_{33} - I_{11}) \quad (13b)$$

$$I_{33}(\ddot{\psi} - \Omega\dot{\phi}) + (I_{22} - I_{11})(\Omega^2\psi + \Omega\dot{\phi}) = 0 \quad (13c)$$

In linearized form, Eq. (13b) shows that the pitch motion of the TCS can be decoupled from the other two Euler angle motions. This allows the pitch motion to be controlled directly through manipulation of the inertia matrix components. For this simulation the control variable is defined as the change in length rate  $\delta\dot{L}$ . The change in length  $\delta L$  is assumed to have only small variations from the reference length  $L_r$ . Substituting Eq. (8) and Eq. (9) and using  $L = L_r + \delta L$  and

$\dot{L} = \delta\dot{L}$ , the equations of motion can be further reduced to the form

$$\ddot{\psi} + \frac{\Omega^2(l_1^2 - l_2^2)}{(l_1^2 + l_2^2)}\psi - \frac{2\Omega\dot{\phi}l_2^2}{(l_1^2 + l_2^2)} = 0 \quad (14a)$$

$$\ddot{\theta} + k\theta + \frac{2L_r\Omega\delta\dot{L}}{(L_r^2 + 2l_1^2)} = 0 \quad (14b)$$

$$\ddot{\phi} - \frac{4\Omega(2l_2^2 - L_r^2)}{(2l_2^2 + L_r^2)}\phi + \Omega \left[ \frac{\dot{\psi}(2l_2^2 - L_r^2)}{(2l_2^2 + L_r^2)} - \psi \right] = 0 \quad (14c)$$

where  $k$  is a constant based on the geometry of the nominal TCS and the orbit by

$$k = \frac{3\Omega^2(L_r^2 - 2l_1^2)}{(L_r^2 + 2l_1^2)} \quad (15)$$

As shown in Eq. (14a) and Eq. (14c), the linearized yaw and roll differential equations are decoupled from the length change parameter  $\delta L$  as well as the pitch motion  $\theta$  and are consequently not driven by the change in geometry control strategy. Without any control input ( $\delta\dot{L} = 0$ ) and using the inertia criteria defined earlier the pitch equation resembles a stable undamped spring-mass system. The control input to asymptotically stabilize Eq. (14b) is<sup>40</sup>

$$u = \delta\dot{L} = C_1\beta\theta - C_2\beta\delta L \quad (16)$$

where  $C_1$  and  $C_2$  are constant feedback gains. The constant  $\beta$  is based on the geometry of the nominal TCS and the orbit through the relationship

$$\beta = \frac{L_r^2 + 2l_1^2}{2\Omega L_r} \quad (17)$$

Natarajan and Schaub in Reference 16 stabilized the pitch motion of a two craft free-flying system by controlling the separation distance. Through feedback on the separation distance of the spacecraft, this control methodology required precise charge level control. Precise charge control can be challenging to achieve because of the changing space plasma environment. The control parameter for the TCS scenario is the change in length rate  $\delta\dot{L}$  with feedback on the pitch angle itself and the change in length  $\delta L$ . A vital difference with this control technique is that precise charge control is not required. The charge of each node of the TCS must merely be greater than a threshold required for each tether to be in tension. The charge can be increased above this value and held constant for the maneuver duration without effect on the control of pitch angle. The resulting state-space representation of the linear closed loop system response is expressed as

$$\begin{bmatrix} \dot{\theta} \\ \ddot{\theta} \\ \delta\dot{L} \end{bmatrix} = \begin{bmatrix} 0 & 1 & 0 \\ -k & -C_1 & C_2 \\ 0 & C_1\beta & -C_2\beta \end{bmatrix} \begin{bmatrix} \theta \\ \dot{\theta} \\ \delta L \end{bmatrix} \quad (18)$$

The feedback gains  $C_1$  and  $C_2$  must be chosen such that the state matrix in Eq. (18) yields eigenvalues with negative real parts.

#### Positive Tension Enforcement

For a given set of initial conditions the equations of motion of the TCS are numerically integrated and the pitch angle is controlled by changing the tether lengths to nodes 1 and 2. It is necessary to calculate the resulting tether forces required to maintain the desired TCS configuration and act like a rigid structure. Desired light-weight tethers are incapable of supporting compressive loads. With these forces known it is possible to set a desired node charge to increase the repulsive forces between nodes and ensure all tethers are in tension. The inertial acceleration of each node and the influence of each tether force and Coulomb force are expressed through Newton's equation of motion as

$$\ddot{\mathbf{R}}_i = -\frac{\mu}{R_c^3}\mathbf{R}_i + \sum_{j=1}^N K_{ij} \frac{T_{ij}\hat{\mathbf{r}}_{ij}}{m_i} + \sum_{j=1}^N \frac{k_c q_i q_j (\mathbf{r}_i - \mathbf{r}_j)}{m_i r_{ij}^3} e^{-r_{ij}/\lambda_d}, \quad i \neq j \quad (19)$$

where  $\mu = 3.986 \times 10^{14} \text{ m}^3\text{s}^{-2}$  is the gravitational coefficient for Earth,  $\mathbf{R}_i$  is the inertial position of each node,  $\mathbf{r}_i$  is the position of each node relative to the CM,  $N$  is the total number of nodes in the TCS model,  $k_c$  is the Coulomb constant, and  $q_i$  are the spacecraft charges. Note that these charges do not influence the relative motion. They simply provide internal pressure to change the tether tensions. The unit direction vector from node  $i$  to  $j$  is  $\hat{\mathbf{r}}_{ij}$ , and  $T_{ij}$  is the tether tension acting on node  $i$  from node  $j$ . The scalars  $K_{ij}$  are the tether connection matrix components which define which nodes are connected by a tether. The six node, twelve tether model shown in Figure 8 has the connection matrix

$$[K] = \begin{bmatrix} 0 & 0 & 1 & 1 & 1 & 1 \\ 0 & 0 & 1 & 1 & 1 & 1 \\ 1 & 1 & 0 & 1 & 0 & 1 \\ 1 & 1 & 1 & 0 & 1 & 0 \\ 1 & 1 & 0 & 1 & 0 & 1 \\ 1 & 1 & 1 & 0 & 1 & 0 \end{bmatrix} \quad (20)$$

If two corresponding nodes are not connected then there is no contributing tether force and the zero value in  $[K]$  is used. With a TCS made up of  $N$  nodes there is a total of  $N$  vector equations of motion shown in Eq. (19). Each of these inertial vector equations is broken down to a set of three orthonormal  $(x, y, z)$  equations resulting in a total of  $3N$  equations. Let us define  $\mathbf{a}_i$  as the sum of the following acceleration terms

$$\mathbf{a}_i = \ddot{\mathbf{R}}_i + \frac{\mu}{R_c^3}\mathbf{R}_i - \sum_{j=1}^N \frac{k_c q_i q_j (\mathbf{r}_i - \mathbf{r}_j)}{m_i r_{ij}^3} e^{-r_{ij}/\lambda_d}, \quad i \neq j \quad (21)$$

which can be expressed in inertial frame components for all  $N$  nodes using

$$[a] = [\mathbf{a}_1^T, \mathbf{a}_2^T, \dots, \mathbf{a}_N^T]^T \quad (22)$$

With a  $N$  node TCS the total number of possible tethers is

$$M = \frac{N(N-1)}{2} \quad (23)$$

In order to solve for each tether tension  $T_{ij}$ , a vector is defined as

$$[T] = [T_{12}, T_{13}, \dots, T_{(N-2)N}, T_{(N-1)N}]^T \quad (24)$$

The  $3N \times M$  matrix  $[B]$  relates the tether tensions  $T_{ij}$  to the  $3N \times 1$  matrix  $[a]$ .

$$[a] = [B][T] \quad (25)$$

where  $[B]$  is defined as

$$[B] = \begin{bmatrix} \frac{K_{12}}{m_1} (\hat{\mathbf{r}}_{12} \cdot \hat{\mathbf{n}}_x) & \frac{K_{13}}{m_1} (\hat{\mathbf{r}}_{13} \cdot \hat{\mathbf{n}}_x) & \dots & \frac{K_{(N-1)N}}{m_1} (\hat{\mathbf{r}}_{(N-1)N} \cdot \hat{\mathbf{n}}_x) \\ \frac{K_{12}}{m_1} (\hat{\mathbf{r}}_{12} \cdot \hat{\mathbf{n}}_y) & \dots & \dots & \dots \\ \vdots & \dots & \dots & \dots \end{bmatrix} \quad (26)$$

where  $\hat{\mathbf{n}}_i$  are the inertial frame unit direction vectors. Using a minimum norm inverse, the set of tether tension with the smallest magnitudes is found:

$$[T] = [B]^\dagger [a] \quad (27)$$

Note that for Eq. (25) to be invertible, the TCS must contain a sufficient number of tethers to make  $[B]$  full rank. While this equations solves for  $M$  tensions, if  $K_{ij} = 0$  then this formula will also yield  $T_{ij} = 0$ . The methodology to compute the TCS tensions is general enough to work for concepts with a general number of nodes. This  $[T]$  matrix must be found subject to the inequality constraint

$$T_{ij} > 0 \quad (28)$$

At each simulation time step, the current minimum nodal charge required for each of the tether forces to be in positive tension can be solved through numerical iterations. With a given required minimal nodal charge it is possible to compute the corresponding required voltage potential using Eq. (2) and the power requirements of each node is computed using Eq. (3). It is shown in Reference 10 that the power requirements of a Coulomb controlled spacecraft are dependent on the spacecraft charge and the space plasma environment. For this example the spacecraft is assumed to be in a sunlit environment and is being charged to a positive potential by emitting electrons. Each spacecraft node is of spherical shape with a diameter of 1 m.

#### *Numerical Simulation*

The following numerical simulation is performed for the modeled TCS using the complete nonlinear equations of motion in Eq. (14) with the linear shape rate  $\delta \dot{L}$  control in Eq. (16).

The control parameter constants are selected based on the linearized closed loop response. The  $C_1$  damping feedback gain value is selected taking into consideration a desired system response settling time of approximately one orbit duration ( $\approx 24$  hrs). The  $C_2$  gain is introduced to drive the steady state change in node length  $\delta L$  to zero. Its value is selected such that the magnitude in the change of length is approximately equal to the pitch angle magnitude change in degrees. The set of initial conditions shown in Table 3 are used with the TCS model to demonstrate the performance characteristics achievable.

**Table 3. Attitude initial conditions used for simulation example case**

Simulation Initial Conditions		Value
Change in length (m)	$\delta L(0)$	0
Yaw angle (deg)	$\psi(0)$	-5
Pitch angle (deg)	$\theta(0)$	-10
Roll angle (deg)	$\phi(0)$	5
Angular rate (deg/s)	$[\omega_1, \omega_2, \omega_3]$	0

Figure 9 shows the resulting motion of the TCS 3-2-1 Euler angles for the given set of initial conditions. As can be seen the initial pitch angle offset of  $-10^\circ$  is controlled towards zero over the duration of approximately one orbit. The uncontrolled yaw and roll angles remain oscillatory but bounded as expected from the linear stability analysis. In order to control the pitch angle with these system response characteristics the required change in node length is also shown. For the initial outer node distance of 20 meters, nodes 1 and 2 will need to increase an additional 3.29 meters from the CM along the  $\hat{b}_3$  body axis direction before returning to zero. This is a realistic tether length change and could be accommodated with a simple tether reel system over the duration of one orbit.

Assuming no charges on the nodes, Figure 10(a) shows the required tether tensions needed at any time step to maintain the time varying TCS shape. Only 6 tension values are shown for the 12 tether system due to the symmetry of the modeled TCS. The tethers connecting the inner central nodes (3,4,5, and 6) are in compression (negative values) due to the out-of-plane relative motion trying to compress the structure. The tethers connecting the outer radial nodes (1 and 2) are under tension and experience slight oscillatory loads due to the reorientation and controlled morphing of the TCS.

The next step is to calculate the node charge required that will produce a set of positive tensions satisfying the inequality condition  $T_{ij} > 0$ . Assuming all nodes are charged to a common level  $q = q_i$ , Figure 10(b) shows the time varying minimum charge levels required to satisfy  $T_{ij} > 0$  at all times. Also shown is the maximum charge level required of  $0.164 \mu\text{C}$ . If the craft are charged to this value or higher, indicated through the shaded region in Figure 10(b), then positive tensions are guaranteed.

For practical purposes it would be beneficial to have all nodes charged to an equivalent potential that remains fixed throughout the maneuver duration. It is not necessary to have precise time-varying charge control as each node can be set to a charge above this maximum value and in the shaded region, ensuring all

tethers are in tension. The maximum tension in the tethers under this induced charge is still relatively low and achievable with current tether materials.

In a sunlit GEO environment with positive spacecraft charging and with each node having a radius of  $\rho_i = 0.5$  m the voltage required is 2.95 kV with a power usage of 42.93 mW necessary to maintain this potential. For this modeled TCS with 6 nodes that equates to a total power of 0.26 W. What is important to note is the required node potential of  $\approx 3$  kV is obtainable on orbit naturally from the surrounding plasma environment under sunlight conditions.<sup>23,24,25</sup>

## Conclusion

The tethered Coulomb structure concept proposed and discussed in this paper offers promising prospects. Thin tethers form a spider-like web between charged spacecraft components which can change the structure's shape by simply changing the tether lengths. The resulting electrostatic repulsion provides an inflationary force which maintains positive tether tension and compensates for differential gravitational or other disturbance forces. The TCS does require operating environments in which the Debye length is large enough to allow inter-spacecraft Coulomb force interaction, which range from the GEO environment through to deep space.

Compared to traditional tether systems, the TCS allows for general three-dimensional structures to be developed without requiring particular equilibrium orientations or spinning to maintain tension. Highly fuel efficient micro-Newton thruster mechanisms can be used to control both the spacecraft charge and shape control, as well as provide small inertial thrust to produce small TCS attitude control torques. The shape control is very fuel efficient, avoids any exhaust plume impingements, and would only require Watt-levels of electrical power. With tether reel mechanisms a large structure can easily be deployed from a compact launch configuration. Similarly, the Coulomb force concept can be safely used for drone deployment and soft docking formation operations from the TCS.

The TCS system modeled here illustrates how shape control can be exploited for novel attitude control. The simulation shows that a TCS dozens of meters in size would require charge levels comparable to what occurs naturally in GEO environment. As an advantage over similar spacecraft formation studies conducted with free flying Coulomb craft, the TCS does not require precise charge control, it merely needs sufficient charge to ensure tension on all tethers.

Future work will delve into the specific use of tethers which includes; materials, dynamic properties and reel mechanisms and shape control. The simulation developed here allows rapid modeling of TCS systems of any number of nodes, size and shape to conduct future studies into potential space bound formations and their direct application. Lab-based vehicles that incorporate Coulomb motion control are under development to commence prototyping of TCS hardware. In summary, the proposed TCS concept is an exciting technology that may expand the possibilities of future formation flight missions.

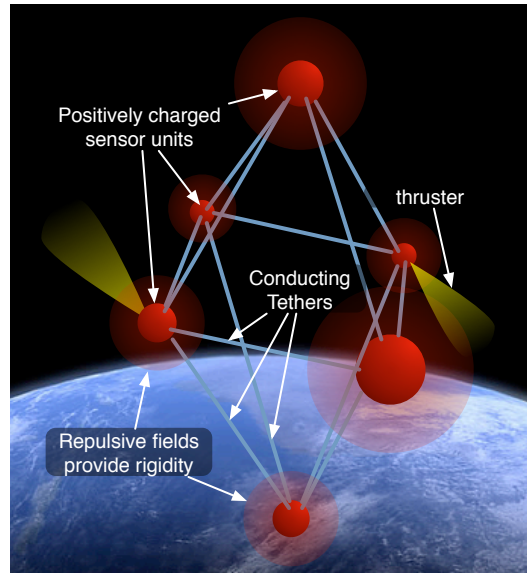
## Acknowledgment

The authors would like to thank Dr. G. G. Parker and Dr. L. B. King at the Michigan Technological University for the fruitful discussions on the TCS concept, as well as the reviewers for their thoughtful feedback.

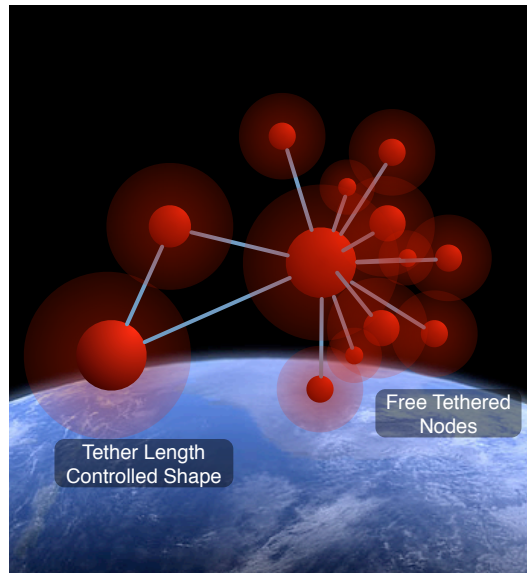
## References

- [1] B. D. Tapley, S. Bettadpur, J. C. Ries, P. F. Thompson, and M. M. Watkins, "GRACE Measurements of Mass Variability in the Earth System," *Science*, Vol. 305, No. 5683, 2004, pp. 503–505.
- [2] T. A. Mulder, "Orbital Express Autonomous Rendezvous and Capture Flight Operations," *AAS/AIAA Spaceflight Mechanics Meeting*, Galveston, TX, Jan. 27–31 2008. Paper AAS 08–209.
- [3] J.-N. Juang, "Controllability and Observability of Large Flexible Spacecraft in Noncircular Orbits," *AIAA Journal of Guidance, Control, and Dynamics*, Vol. 3, March–April 1980, pp. 186–188.
- [4] J. L. Junkins and Y. Kim, *Introduction to Dynamics and Control of Flexible Structures*. Washington D.C.: AIAA Education Series, 1993.
- [5] M. D. Rhodes, R. W. Will, and M. A. Wise, "A telerobotic system for automated assembly of large space structures," Technical Report NASA-TM-101518, Langley Research Center, March 1 1989.
- [6] V. J. Modi, G. Chang-Fu, A. K. Misra, and D. M. Xu, "On the Control of the Space Shuttle Based Tethered Systems," *Acta Astronautica*, Vol. 9, No. 6, 1982, pp. 437–443.
- [7] A. Mazzoleni, "End-Body Dynamics of Artificial-Gravity-Generating Tethered Satellite System During Non-Planar Spin-Up with Elastic Effects Included," *AAS/AIAA Astrodynamics Specialist Conference*, Big Sky, Montana, August 2003. Paper No. 03–537.
- [8] S. G. Tragesser and A. Tuncay, "Orbital Design of Earth-Oriented Tethered Satellite Formations," *Journal of the Astronautical Sciences*, Vol. 53, Jan. – March 2005, pp. 51–64.
- [9] C. Menon and C. Bombardelli, "Self-Stabilising Attitude Control for Spinning Tethered Formations," *Acta Astronautica*, Vol. 60, 2007, pp. 828–833.
- [10] L. B. King, G. G. Parker, S. Deshmukh, and J.-H. Chong, "Spacecraft Formation-Flying using Inter-Vehicle Coulomb Forces," tech. rep., NASA/NIAC, January 2002. <http://www.niac.usra.edu>.
- [11] C. D. Brown, *Spacecraft Propulsion*. AIAA Education Series, 1996.
- [12] J. Berryman and H. Schaub, "Static Equilibrium Configurations in GEO Coulomb Spacecraft Formations," *AAS/AIAA Spaceflight Mechanics Meeting*, Copper Mountain, CO, Jan. 23–27 2005. Paper No. AAS 05–104.
- [13] J. Berryman and H. Schaub, "Analytical Charge Analysis for 2- and 3-Craft Coulomb Formations," *AIAA Journal of Guidance, Control, and Dynamics*, Vol. 30, Nov.–Dec. 2007, pp. 1701–1710.
- [14] H. Vasavada and H. Schaub, "Analytic Solutions for Equal Mass Four-Craft Static Coulomb Formation," *Journal of the Astronautical Sciences*, Vol. 56, Jan. – March 2008, pp. 7–40.
- [15] A. Natarajan and H. Schaub, "Hybrid Control of Orbit Normal and Along-Track 2-Craft Coulomb Tethers," *AAS/AIAA Spaceflight Mechanics Meeting*, Sedona, AZ, Jan. 28–Feb. 1 2007. Paper AAS 07–193.
- [16] A. Natarajan and H. Schaub, "Linear Dynamics and Stability Analysis of a Coulomb Tether Formation," *AIAA Journal of Guidance, Control, and Dynamics*, Vol. 29, July–Aug. 2006, pp. 831–839.
- [17] A. Natarajan and H. Schaub, "Orbit-Nadir Aligned Coulomb Tether Reconfiguration Analysis," *AAS/AIAA Spaceflight Mechanics Meeting*, Galveston, TX, Jan. 27–31 2008. Paper AAS 08–149.
- [18] A. Natarajan, H. Schaub, and G. G. Parker, "Reconfiguration of a Nadir-Pointing 2-Craft Coulomb Tether," *Journal of British Interplanetary Society*, Vol. 60, June 2007, pp. 209–218.
- [19] I. I. Hussein and H. Schaub, "Stability and Control of Relative Equilibria for the Three-Spacecraft Coulomb Tether Problem," *AAS/AIAA Astrodynamics Specialist Conference*, Mackinac Island, MI, Aug. 19–23 2007. Paper AAS 07–269.
- [20] R. E. Freeland, G. D. Bilyeu, G. R. Veal, and M. M. Mikulas, "Inflatable Deployable Space Structures Technology Summary," *49th International Astronautical Congress*, Melbourne, Australia, Sept. 28 – Oct. 2 1998.

- [21] R. G. Cobb, S. N. Lindemuth, J. C. Slater, and M. R. Maddux, "Development and Test of a Rigidizable Inflatable Structure Experiment," *45th AIAA/ASME/ASCE/AHS/ASC Structures, Structural Dynamics & Materials Conference*, Palm Springs, CA, April 19–22 2004. Paper No. AIAA 2004–1666.
- [22] P. A. Tarazaga, D. J. Inman, and W. K. Wilkie, "Control of a Space Rigidizable Inflatable Boom Using Macro-fiber Composite Actuators," *Journal of Vibration and Control*, Vol. 13, No. 7, 2007, pp. 935–950.
- [23] C. P. Escoubet, M. Fehringer, and M. Goldstein, "The Cluster Mission," *Annales Geophysicae*, Vol. 19, No. 10/12, 2001, pp. 1197–1200.
- [24] K. Torkar and et. al., "Spacecraft Potential Control aboard Equator-S as a Test for Cluster-II," *Annales Geophysicae*, Vol. 17, 1999, pp. 1582–1591.
- [25] K. Torkar, W. Riedler, and C. P. Escoubet, "Active Spacecraft Potential Control for Cluster – Implementation and First Results," *Annales Geophysicae*, Vol. 19, No. 10/12, 2001, pp. 1289–1302.
- [26] D. R. Nicholson, *Introduction to Plasma Theory*. Malabar, FL: Krieger, 1992.
- [27] C. C. Romanelli, A. Natarajan, H. Schaub, G. G. Parker, and L. B. King, "Coulomb Spacecraft Voltage Study Due to Differential Orbital Perturbations," *AAS/AIAA Spaceflight Mechanics Meeting*, Tampa, FL, Jan. 22–26 2006. Paper No. AAS-06-123.
- [28] M. Tajmar and W. S. a. A. Genovese, "Indium FEED Thruster Beam Diagnostics, Analysis and Simulation," *37th AIAA/ASME/SAE/ASEE Joint Propulsion Conference and Exhibit*, Salt Lake City, UT, July 8–11 2001. Paper No. AIAA 01-34440.
- [29] V. Hruba, M. Gamero-Castano, P. Falkos, and S. Shenoy, "Micro Newton Colloid Thruster System Development," *27th International Electric Propulsion Conference*, Pasadena, CA, Oct. 15–10 2001. IEPC Paper No. 01-281.
- [30] K. Torkar and e. al, "Spacecraft Potential Control using Indium Ion Source – Experience and Outlook Based on Six Years of Operation in Space," *6th Spacecraft Charging Control Technology Conference*, Hanscom AFB, MA, Sept. 2000. AFRL-VS-TR-20001578.
- [31] J. M. Makela and L. B. King, "Progress on Re-generable Field Emission Cathodes for Low-Power Electric Propulsion," *30 International Electric Propulsion Conference*, Florence, Italy, Sept. 17–20 2007. IEPC-2007-152.
- [32] R. E. Freeland, G. D. Bilyeu, G. R. Veal, M. D. Steiner, and D. E. Carson, "Large Inflatable Deployable Antenna Flight Experiment Results," *Acta Astronautica*, Vol. 41, No. 4–10, 1997, pp. 267–277.
- [33] R. D. Robinett, G. G. Parker, H. Schaub, and J. L. Junkins, "Lyapunov Optimal Saturated Control for Nonlinear Systems," *AIAA Journal of Guidance, Control, and Dynamics*, Vol. 20, Nov.–Dec. 1997, pp. 1083–1088.
- [34] J. C. Mankins, "A Fresh Look at Space Solar Power: New Architectures, Concepts and Technologies," *Acta Astronautica*, Vol. 41, Aug. 1997, pp. 347–359.
- [35] J. A. Carroll, "Space Transportation Development Using Orbital Debris," tech. rep., Tether Applications, Inc., Chula Vista, CA, December 2002.
- [36] J. A. Carroll and J. C. Oldson, "Tethers for Small Satellite Applications," *AIAA/USU Small Satellite Conference*, Logan, Utah, 1995.
- [37] M. Nohmi, "Attitude control of a tethered space robot by link motion under microgravity," *Control Applications, 2004. Proceedings of the 2004 IEEE International Conference on*, Vol. 1, 2-4 Sept. 2004, pp. 424–429 Vol.1.
- [38] J. Valverde, J. L. Escalona, J. Mayo, and J. Dominguez, "Dynamic Analysis of a Light Structure in Outer Space: Short Electrodynamical Tether," *Multibody Systems Dynamics*, Vol. 10, 2003, pp. 125–146.
- [39] H. Schaub and J. L. Junkins, *Analytical Mechanics of Space Systems*. Reston, VA: AIAA Education Series, October 2003.
- [40] G. F. Franklin, J. D. Powell, and A. Emami-Naeini, *Feedback Control of Dynamic Systems*. Upper Saddle River, NJ: Pearson Prentice Hall, 2006.



(a) Tall and slender tethered Coulomb structure utilizing gravity gradients to stabilize orientation.



(b) Hybrid TCS concept with fixed shape component and free tethered nodes.

**Figure 3. TCS Concept Illustrations.**

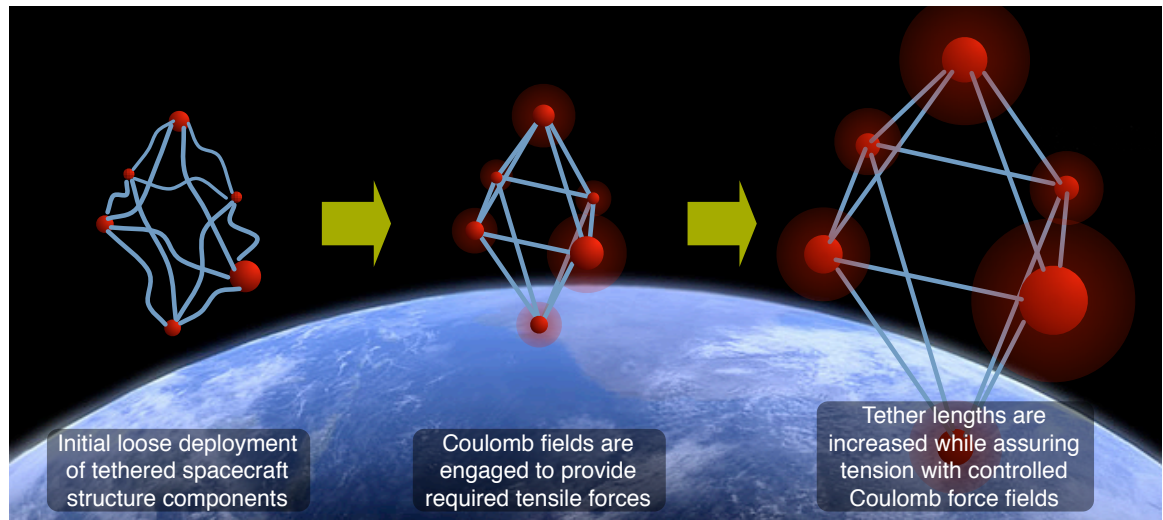
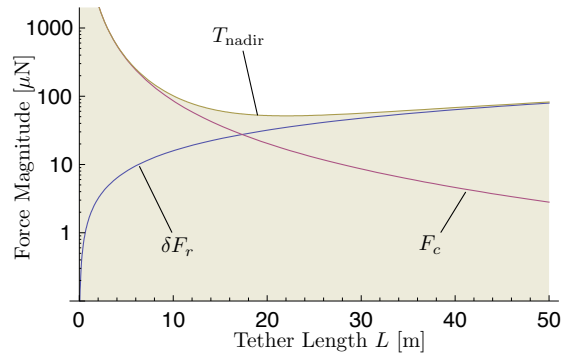
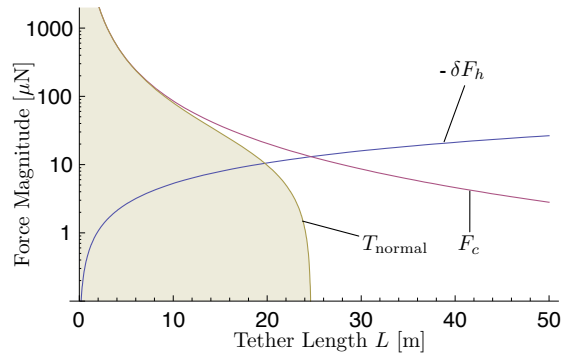


**Figure 4. Illustration of a tethered Coulomb structure being first deployed, and then inflated to a larger size.**

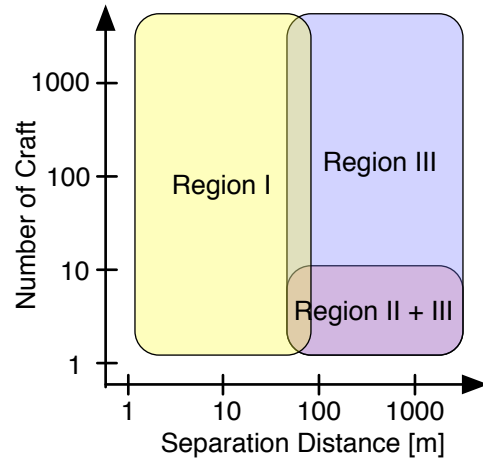


(a) Orbit Radial Deployment

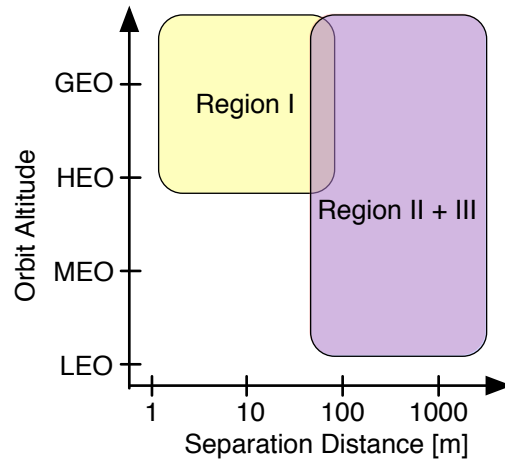


(b) Orbit Normal Deployment

**Figure 5. Comparison of the Coulomb and Differential Gravity Force Magnitude and Resulting Tether Tension for GEO 2-Craft TCS with 100 kg nodes and  $1\mu\text{C}$  Charge.**



(a) Scalability of number of craft and component separation distances



(b) Operating altitudes and separation distances

**Figure 6. Operating regime comparisons between TCS concept (region I), free-flying spacecraft cluster (region II), and a tethered structured with micro-thrusters maintaining tension (region III).**

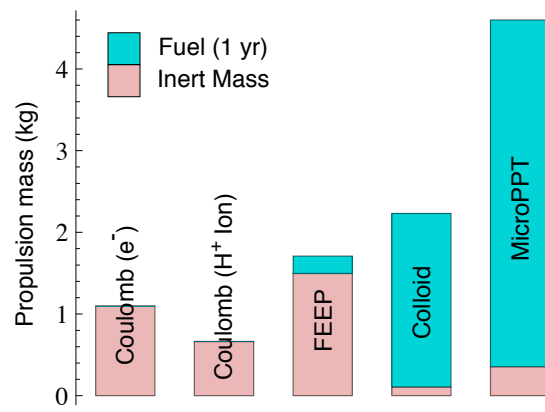
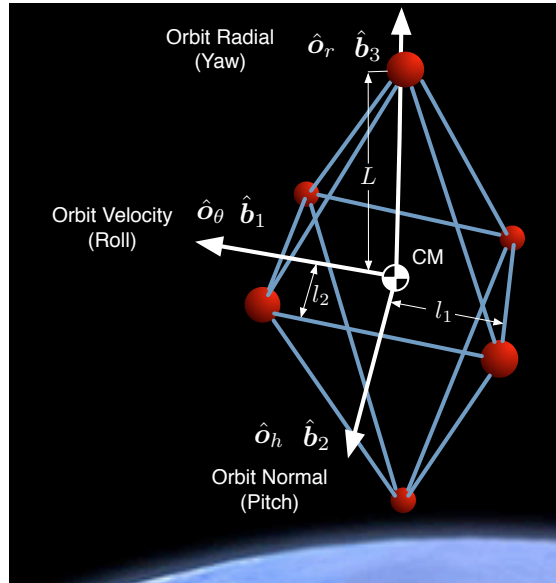
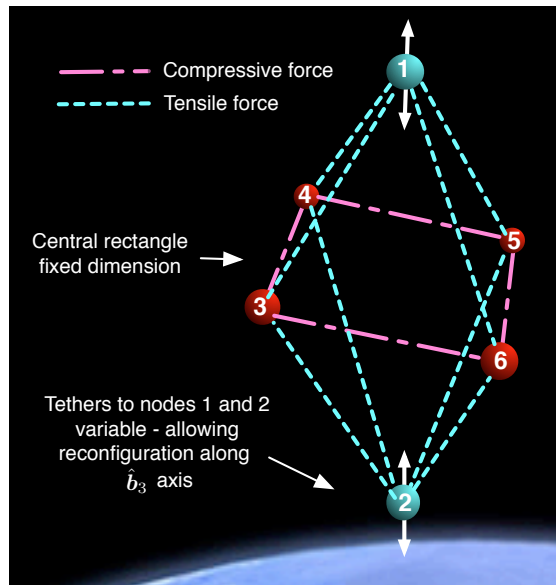


Figure 7. Propulsion mass comparison for a 10 node tethered structure (25 meter nominal separation) over 1 year.



(a) CTS model dimensions, orbit axis and 3-2-1 Euler angle definition (shown with zero attitude rotation)



(b) CTS model showing zero attitude, natural (un-charged) internal tether forces and reconfigurable outer nodes

**Figure 8. Six node TCS model with axes definition, internal tether forces, and node numbering.**

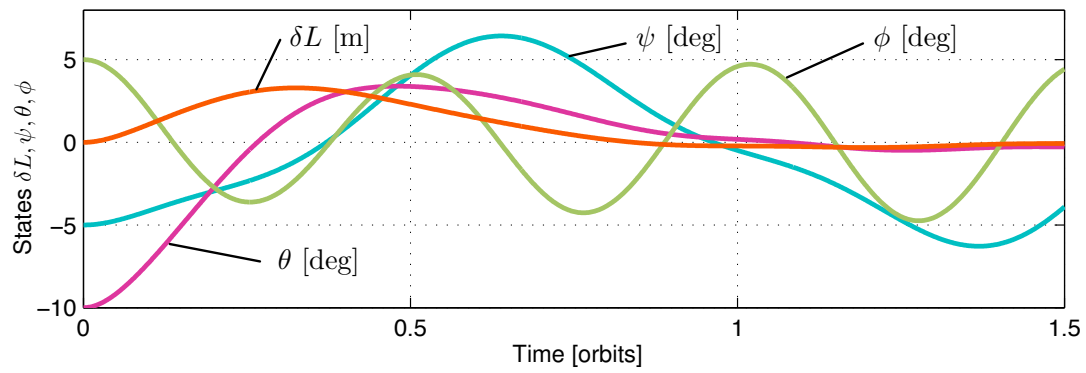
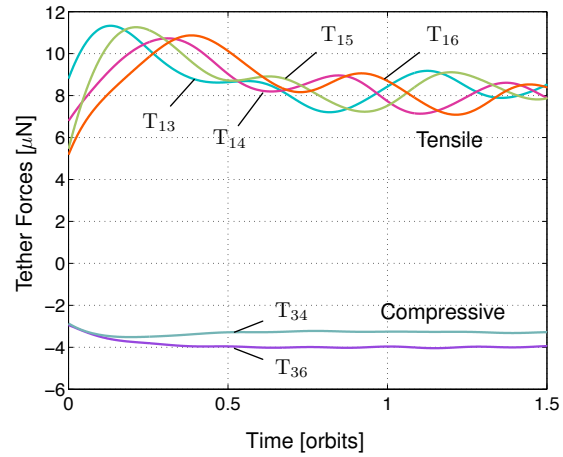
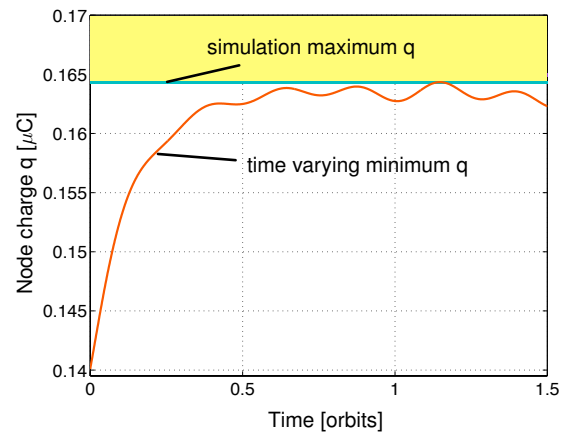


Figure 9. Control simulation Euler angles and change in outer node tether length.



(a) Un-charged tether internal forces during simulation



(b) Charge required to ensure tension in all tethers during simulation

**Figure 10. Tether forces and node charge requirements**